

Research Article

Empirical Modeling of Cancer Cell Viability in Oxygen-Mediated Photodynamic Therapy

Kuo-Ti Chen¹, Jui-Teng Lin², Hsia-Wei Liu^{3*}

¹Graduate Institute of Applied Science and Engineering, Fu Jen Catholic University, New Taipei City, Taiwan, Republic of China

²New Vision Inc. Taipei, Taiwan, Republic of China

³Department of Life Science, Fu Jen Catholic University, New Taipei City, Taiwan, Republic of China

*Corresponding Author

Dr. Hsia-Wei Liu, Department of Life Science, Fu Jen Catholic University, New Taipei City, Taiwan, Republic of China, E-mail: 079336@gmail.com

Received: 15 August 2019;

Accepted: 12 September 2019;

Published: 01 October 2019

Abstract

The dynamic roles of photosensitizer (PS) concentration and light intensity were measured and analyzed empirically. The efficacy of photodynamic therapy (PDT) and cell viability (CV) are measured (in vitro) and analyzed by analytic and numerical modeling. For a fixed PS concentration, CV is a nonlinear decreasing function of light intensity and exposure time; for a fixed light intensity, higher PS concentration achieves higher efficacy or smaller CV (at steady-state), in consistent to our analytic formulas. The anticancer efficacy may be improved by various strategies such as resupply of Ce6, external oxygen, or stabilizing the singlet oxygen (with increased lifetime).

Keywords: Photodynamic therapy; Oxygen-mediated; Cancer therapy; Efficacy; Cell viability

Citation: Kuo-Ti Chen, Jui-Teng Lin, Hsia-Wei Liu. Empirical Modeling of Cancer Cell Viability in Oxygen-Mediated Photodynamic Therapy. Journal of Cancer Science and Clinical Therapeutics 3 (2019): 143-151.

1. Introduction

Radical-mediated photopolymerization has two major processes [1,2]: (i) type-I for crosslinking (or gelation) of biomaterials using radical-substrate coupling; and (ii) type-II for photodynamic therapy (PDT) using light-initiated oxygen free radicals. Photopolymerization offers various applications in dermatology, dental, orthopedics (tissue engineering), ophthalmology, anti-cancer and anti-microbial [3-10]. Oxygen plays a critical role in the efficacy of Type-II PDT, where oxygen consumption and diffusion effects in PDT was first reported by Foster et al [1] and was updated and reviewed recently by Zhu et al [9] in 2017. The kinetics of both oxygen-mediated (type-II) and non-oxygen-mediated (type-I) was reported by Lin recently [11]. Photochemical kinetics for the efficacy of PDT is analyzed to show the critical factors of efficacy including: the concentrations of photosensitizers and oxygen in the treated target, the exposure time, intensity and dose (energy) of the light applied to the target. Higher light intensity has faster rising curve of the efficacy, but it reaches the same steady-state value as that of low intensity. Higher initial concentration of oxygen and photosensitizers, C_0 , always provide higher efficacy. Minimum light dose and/or less exposure time for accelerated procedure by using a higher intensity (but same dose, E_0) are desired. Threshold product of drug-light dose $[C_0E_0]^*$ is derived showing that larger C_0 has a lower E_0^* and vice versa [13]. However, higher intensity requires a higher threshold energy, and does not follow the Bunsen-Roscoe law (BRL) of reciprocity, when there is an oxygen source term [11]. Effort to minimize side effects of PDT at high light intensity, various modified PDT protocols have been explored involving

reduced PS dosage, laser fluence, or a combination of both [13-15].

Our previous studies presented detail of the kinetics and efficacy for type-I and type-II photodynamic mechanism [11]. We have also presented the improvement of anti-cancer efficacy by synergistic effects of PDT and photothermal therapy (PTT) [16-18]. The role of concentration of PS and oxygen, rate constant, oxygen external source term, light dose, intensity and exposure time in the efficacy and threshold dose of anti-cancer was theorized [12] and a drug-light dose law was also analyzed for optimal PS concentration [13]. In this study, we will focus the measured profiles of the cell viability (measured in vitro) for various light intensities and PS concentrations, which will be analyzed by our developed formulas and numerical modeling. Finally, we will compare our measured data with that of Klimenko et al [19].

2. Methods

2.1 Experimental setup

The experimental setup is shown in Figure 1, the PS is Chlorine e6 (Ce6) solution at various concentration of 0.00312 to 0.00625 %, and a red diode laser (at 660 nm) with intensity of $I_0 = (51, 102, 203) \text{ mW/cm}^2$. The cell viability (CV) is measured at above described various conditions to study the roles of light intensity (at a fixed Ce6 concentration), and Ce6 concentration (at a fixed light intensity). The referenced initial light intensity is calibrated by its value in pure water solution, where the input laser is collimated and output power is measured after a fixed aperture of 10 mm.

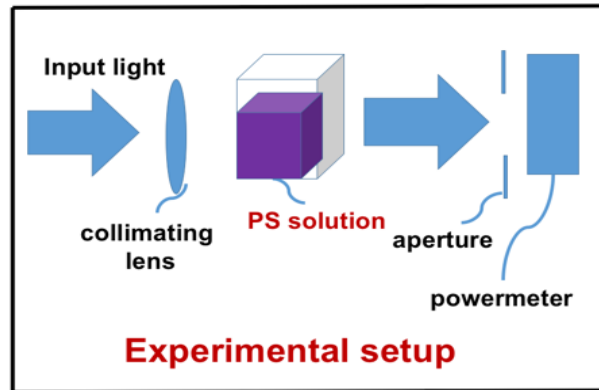


Figure 1: Experimental setup for cells in Chlorine e6 (Ce6) solution with various concentration and exposed to a laser with various intensity.

2.2 Theory and modeling

As shown by Figure 2 for the kinetics of PDT, the Macroscopic kinetic equations were previously developed for the concentration of PS (C), oxygen [O₂], singlet oxygen, X, the target tissue, [A], and the light intensity, I (z, t), under a so-called quasi-steady-state condition are given by [11]

$$\frac{\partial C(z,t)}{\partial t} = -bI(g[A] + kg'C[O_2])C + k'R[O_2] \quad (1.a)$$

$$\frac{\partial X}{\partial t} = k_3[O_2]T - (k_6 + k_{11}C + k_8[A])X \quad (1.b)$$

$$\frac{\partial [O_2]}{\partial t} = -(bICg' + k'R)[O_2] + P \quad (1.c)$$

$$\frac{\partial [A]}{\partial t} = -[bICg(1 + g'[O_2]) + k'R][A] \quad (1.d)$$

where $g = k_7 / (k_3[O_2] + k_7[A] + k_5)$; $g' = k_8 / (k_6 + k_{11}C + k_8[A])$; $b = 83.6a'qw$; w being the UV light wavelength (in cm) and light intensity I (z, t) in mW/cm²; q is the quantum yield of the PS triplet state; Equation (2.f) also includes an oxygen source term given by [14], $P = (1 - [O_2]/O_0)P'$, with a maximum rate constant P', with a maximum rate constant P₀ and

initial oxygen concentration Y₀. This term may be also given by the oxygen diffusion

$P = D_0 \nabla^2 [O]$. All the reaction rate constants are defined by the associated coupling terms.

The dynamic light intensity is given by [10]

$$\frac{\partial I(z,t)}{\partial z} = -A'(z,t)I(z,t) \quad (2.a)$$

$$A'(z,t) = 2.3[(a' - b')C(z,t) + b'C_0 + Q] \quad (2.b)$$

where a' and b' are the extinction coefficients of PS and the photolysis product, respectively; Q is the absorption coefficient of the cancer cells (or tissue) at the UV wavelength.

Solutions of C, [O₂], [X] and I (z, t) provide the anti-cancer efficacy defined by $C_{eff} = 1 - \exp(-S)$, which also provides the formula for cell viability, defined as $CV = 1 - Eff = \exp(-S)$, where the S-function, for the situation that type-II, oxygen-mediated process is predominant, (with $g \ll g'$), is the time integral of the singlet oxygen, which is given by the steady-state of Equation (1.b), or [10,11]

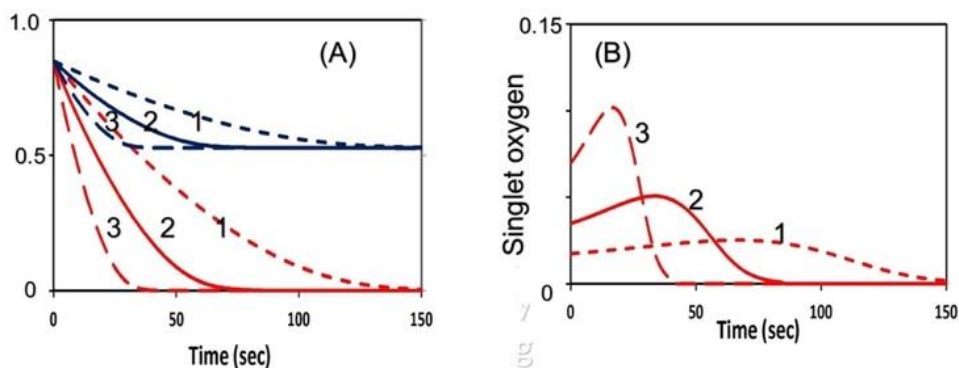


Figure 3: The numerically produced normalized temporal profiles of: (A) oxygen (red curves) and PS concentration (blue curves); (B) singlet-oxygen, for various light intensity of 50, 100, 200 mW/cm², (for curves 1,2,3), without external oxygen source ($p = 0$); $c' = 33$, $k_8[A] = 0.005$ (uM) (for type-II dominant) and for substrate $[A] = 50$ uM.

Figures 3,4 and 5 show the following important features:

- (i) For the same dose, lower light intensity achieves a higher steady-state-efficacy (SSE) in type-I; in contrast to type-II, which has an equal SSE.
- (ii) Type-II process is also affected by the available oxygen. Higher light intensity produces more efficient singlet oxygen, resulting in a higher transient efficacy, in which all intensities reach the same SSE when oxygen is completely depleted. With external oxygen, type-II efficacy increases with time, otherwise, it is governed only by the light dose, i.e., same dose

achieves same efficacy. Moreover, type-II has an efficacy following Bunsen Roscoe law (BRL), whereas type-I follows non-BRL.

- (iii) The photopolymerization dynamics may be defined by the availability of oxygen, where both type-I and -II coexist until the oxygen is depleted. For the case that both type-I and type-II exit, the combined effects lead to a higher efficacy than the case of type-I or type-II only. Oxygen may also play critical role in two competing type-I and type-II processes, in which oxygen inhibits free-radical polymerization thereby reducing type-I crosslink efficiency.

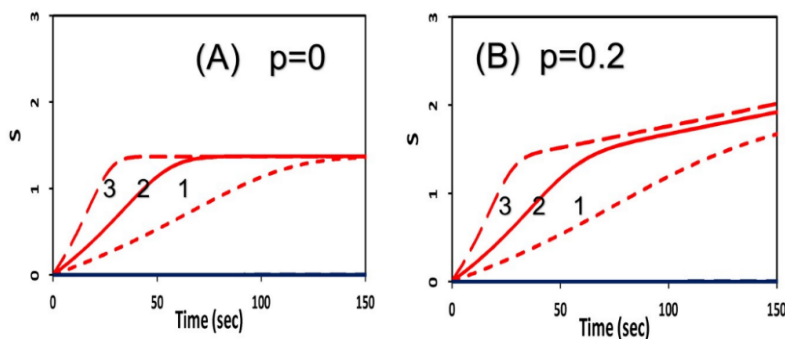


Figure 4: Same as Figure 3, but for the type-II S-function, for the case of without (A), and with (B) external oxygen source, with $p = 0$ and $p = 0.2$ (1/s), respectively.

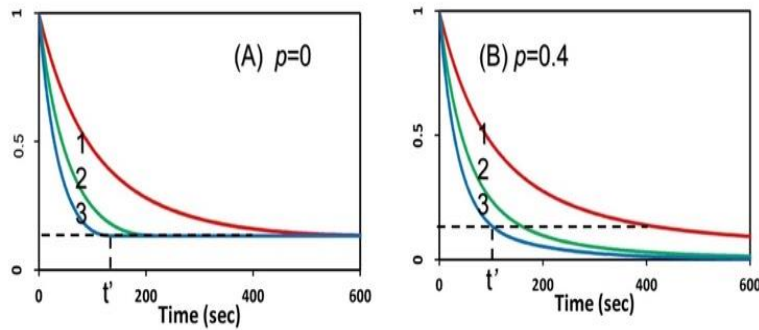


Figure 5: The calculated temporal profiles for cell viability (CV), without (A), and with (B) external oxygen source, for various PS concentration of (5,10,15) uM (for curve 1,2,3), and light intensity of 20 mW/cm²; also shown is the threshold exposure time (t').

3.2 Experimental data

We shall now present our measured data which will be compared and analyzed by our theoretically predicted features discussed earlier. Figure 6 shows the measured dynamic spectra of Chlorine e6 (Ce6) solution under red light exposure at various time. These Ce6 spectra absorption peaks are red-shifted (about 10 nm) after photoinitiated by the red light, besides the reduced peak value due to the bleach (depletion) effect. This effect was also observed by the color change. The measured spectra of Figure 6 also indicate the dynamic feature of the light intensity which is an increasing function of time when the PS concentration is depleted.

Greater details of the dynamic features may be found in Ref.[10], [16].

Figure 7 shows the measured temporal profiles for cell viability for a fixed light intensity of $I_0=50$ mW/cm², and Ce6 concentration $C_0= 0.0031$ and 0.0062 uM. Figure 8 shows the measured and the theoretical results for various light intensity at $I_0= (25,50,100,200)$ mW/cm². We note that the theoretical data are based on type-II S function of Equation (1.b) which is numerically calculated based on the fit effective absorption factor, $A(z, t)$.

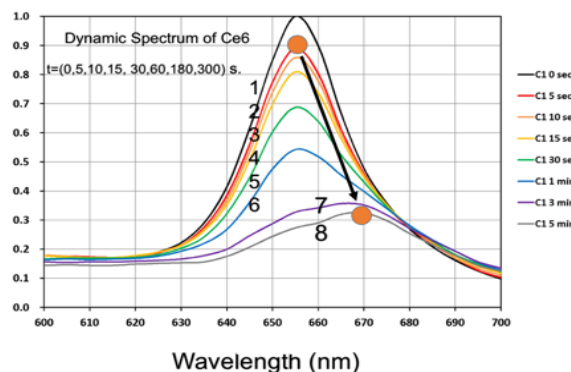


Figure 6: Measured dynamic spectra of Chlorine e6 solution under red light exposure at various time of $t=(0,5,10,15,30,60,160,300)$ seconds, for curves (1,2,3,4,5,6,7).

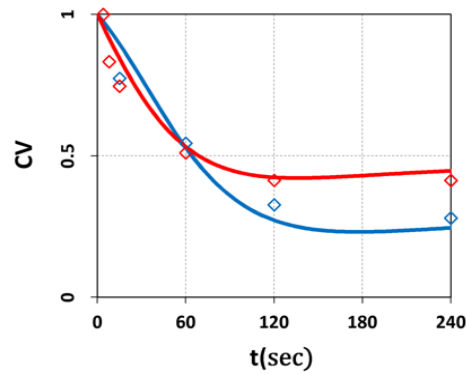


Figure 7: Measured temporal profiles for cell viability for a fixed light intensity of $I_0=50 \text{ mW/cm}^2$, and Ce6 concentration $C_0= 0.0031$ and 0.0062 uM , shown by red and green dots; also shown are the calculated curves in red and green, respectively.

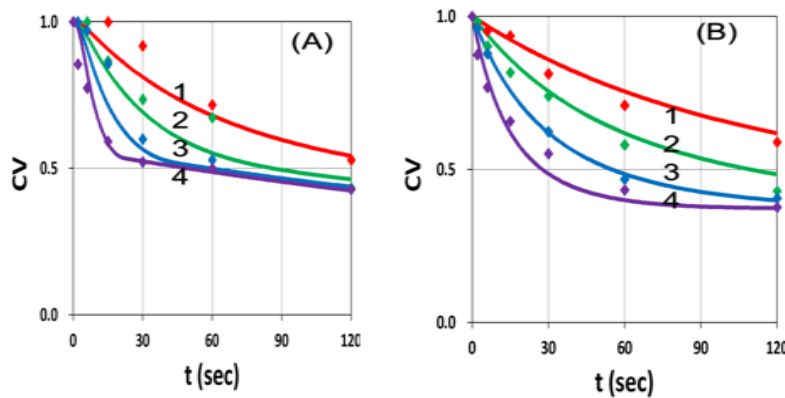


Figure 8: Same as Figure 7, but for Ce6 concentration: (A) $C_0=0.0031 \text{ uM}$ and (B) 0.0062 uM , for various light intensity at $I_0= (25,50,100,200) \text{ mW/cm}^2$, for curve (1,2,3,4).

3.3 Data analysis

The measured data shown by Figure 7 and 8 may be analyzed by our theory as follows. Figure 7 shows that cell viability (CV) is an exponentially decreasing function of the light exposure time (or dose) for a fixed light intensity, and higher PS concentration is more efficient in anti-cancer and has a lower CV. Our theoretical and measured data are comparable to cell viability curves after red-light irradiation of Radachlorin reported in vivo by Klimenko et al [19], in which their Figure 5 may be compared with our Figure 7.

Figure 8 shows that CV, for a fixed Ce6 concentration, is a decreasing function of light intensity, in consistent to our theoretical prediction based on Equation (1.b), and Figure 3 and 4, that high intensity kills the cells faster, but has the same steady-state CV as that of low intensity, when the oxygen is completely depleted and Ce6 concentration reaches its steady-state, as shown by Figure 3(A).

Our empirical modeling demonstrates the following important features:

- (i) Higher light intensity has a faster depletion of oxygen and PS concentration;

(ii) For the same dose, higher light intensity has a faster rising efficacy, but reach the same steady-state as that of low intensity for type-II PDT (for the case of no external oxygen); in contrast to type-I, in which higher light intensity has lower steady-state efficacy;

(iii) The cell viability (CV) at various conditions are measured and shown in Figure 3. For a fixed Ce6 concentration, CV is a nonlinear decreasing function of light intensity and exposure time, in consistent to our formula, $CV = 1 - C_{eff} = \exp(-S)$, with S given by Equation (3).

We should note that the CV and anti-cancer therapy in our in vitro measurements are much less efficient than in vivo having much higher available oxygen from the blood flowing. The anti-cancer efficacy (dominant by type-II mechanism) is limited by the available oxygen and Ce6 in the cell-Ce6-mixed solution. Therefore, it may be enhanced by the resupply of Ce6 and/or external oxygen. The CV reaches its steady-state when

oxygen is completely depleted by the light. Furthermore, increase the lifetime of the singlet oxygen, which is proportional to, as shown by Equation (1.b), $k_3[O_2] T = g g' [O_2]$, with $g = k_7 / (k_5 + k_3[O_2] + k_7[A])$; $g' = k_8 / (k_6 + k_{11}C + k_8[A])$, will improve the anti-cancer efficacy; i.e., smaller k_5 term in g , or stabling the singlet oxygen by an agent such as D_2O , will improve the efficacy. This strategy has been used in corneal crosslinking [10], but not yet in anti-cancer PDT.

4. Conclusion

We have measured the cell viability (CV) in Chlorine e6 (Ce6) solution and under a red diode laser exposure at various time and light intensity. The measured data are in consistent with our theoretically predicted features. Anti-cancer efficacy may be enhanced by the resupply of Ce6, external oxygen, or stabling the singlet oxygen (with an increased lifetime).

References

1. Fouassier JP. Photoinitiation, Photo-Polymerization, and Photocuring: Fundamentals and Applications; Hanser Gardner Publications: Munich, Germany (1995).
2. Odian G. Principles of Polymerization, Fourth ed. John Wiley & Sons, Inc. New York (2006).
3. Chen FM, Shi S. Principles of Tissue Engineering, 4th ed.; Elsevier: New York, NY, USA (2014).
4. Chen FM, Shi S. Principles of Tissue Engineering, 4th ed.; 2014, Elsevier: New York, NY, USA (2014).
5. Pereira R, Bartolo P. Photopolymerizable hydrogels in regenerative medicine and drug delivery. *Top. Biomater* (2014): 6-28.
6. Anseth KS, Klok HA. Click chemistry in biomaterials, nanomedicine, and drug delivery. *Biomacromolecules* 17 (2016): 1-3.
7. Marturano V, Cerruti P, Giamberini M, et al. Light-responsive polymer micro- and nano-capsules. *Polymers* 9 (2017).
8. Qiu M, Wang D, Liang WY, et al. Novel concept of the smart NIR-light-controlled drug release of black phosphorus nanostructure for cancer therapy. *Proc. Natl. Acad. Sci. USA* 115 (2018): 501-506.
9. Zhu TC, Finlay JC, Zhou X, et al. Macroscopic modeling of the singlet oxygen production during PDT. *Proc SPIE* 6427 (2007):6427O81-6427O812.

10. Lin JT, Cheng DC. Modeling the efficacy profiles of UV-light activated corneal collagen crosslinking. *PloS One* 12 (2017): e0175002.
11. Lin JT. Efficacy S-formula and kinetics of oxygen-mediated (type-II) and non-oxygen-mediated (type-I) corneal cross-linking. *Ophthalmology Research* 8 (2018): 1-11.
12. Lin JT, Chen KT, Liu HW. Analysis the role of oxygen, light Intensity, threshold dose and efficacy improvement of anti-cancer via type-II photodynamic therapy. *Nov Appro in Can Study 2* (2018): NACS.000533.
13. Lin JT. Analysis of drug-light dose on the efficacy of photodynamic therapy of age related macular degeneration. *J Ophthalm Studies* 1 (2018).
14. Dhiran NA, Yang Y, Somani S. Long-term outcomes in half-dose verteporfin photodynamic therapy for chronic central serous retinopathy. *Clinical Ophthalmology* 11 (2017): 2145-2149.
15. Cheng CK, Chang CK, Peng CH. Comparison of photodynamic therapy using half-dose of verteporfin or half-fluence of laser light for the treatment of chronic central serous chorioretinopathy. *Retina* 37 (2017): 325-333.
16. Lin JT, Liu HW, Chen KT, et al. Modeling the optimal conditions for improved efficacy and crosslink depth of photo-initiated polymerization. *Polymer* 11 (2019): 217.
17. Lin JT, Chen KT, Liu HW. Novel techniques for improving anti-cancer efficacy via synergistic phototherapy. *Op Acc J Bio Eng & App 2* (2018): OAJBEA.MS.ID.000126.
18. Lin JT. Advances of cancer synergic phototherapy: kinetics and efficacy. *Nov Appro in Can Study 2* (2018): NACS.000529.
19. Klimenko VV, Shmakov SV, Kaydanov NE, et al. In vitro singlet oxygen threshold dose at PDT with Radachlorin. *SPIE Proceedings. Optical Society of America* (2017): 1041703.



open access article distributed under the terms and conditions of the [Creative Commons Attribution \(CC-BY\) license 4.0](https://creativecommons.org/licenses/by/4.0/)